Magnetic hyperfine interactions in amorphous Fe_xB_{100-x}

C. L. Chien and K. M. Unruh
Department of Physics, The Johns Hopkins University, Baltimore, Maryland 21218
(Received 21 December 1981)

Sputtered amorphous Fe_xB_{100-x} has been studied by ^{57}Fe Mössbauer spectroscopy from below the magnetic threshold at $x_c \simeq 38$ through the magnetic region, to $x = 90$. T_C is found to rise sharply with Fe concentration, peaking at $x \simeq 70$, and then to decrease monotonically. Measurements under a small external field indicate that these samples are ferromagnetic. The hyperfine field distributions $\{P(H)\}$ exhibit rather structureless, single-maximum patterns that continuously shift to higher H values as the Fe concentration is increased. The isomer shift, on the other hand, shows a maximum at $x \simeq 50$. The data are discussed in terms of the localized moment and itinerant electron descriptions. It is also shown that several models (e.g., charge-transfer and quasicrystalline models) based on the results from liquid-quench samples with $72 \leq x \leq 86$, are not valid over the wider composition range studied here. The magnetic properties and hyperfine interactions of sputtered and liquid-quench samples are compared in the region of common compositions.

I. INTRODUCTION

Amorphous metallic solids can be made by several well-known methods. The liquid-quench methods, where the random atomic arrangements in the liquid state are frozen through the rapid-quenching process, are perhaps the most widely used.[1,2] However, this technique is successful only for alloys near eutetic compositions, which in the case of transition-metal (T)-metalloid (M) alloys is near $T_{80}M_{20}$.[2]

The amorphous state can also be obtained by vapor deposition techniques in which the random arrival of atoms from the vapor is preserved in the solid state.[3] An important advantage of this method is that amorphous solids over a much wider composition range can be achieved. The availability of amorphous solids over wide ranges in composition allows various magnetic, electrical, structural, etc. properties to be studied as the composition is continuously varied. Therefore, many models based on results from the liquid-quench samples can be more stringently tested.

There are a large number of studies on liquid-quench Fe_xB_{100-x} within the narrow composition range of $72 \leq x \leq 86$.[2,4-6] In addition, there are a few recent studies on vapor-deposited films with much lower Fe contents. Aboaf *et al.* have made samples with $64 \leq x \leq 84$.[7] Blum *et al.* have studied, using Mössbauer spectroscopy, samples with $x = 40$, 45, and 50.[8] Stobiecki *et al.* have studied the transport properties of samples with $25 \leq x \leq 88$.[9] The majority of these samples were made from composite targets of various kinds where pieces of Fe or B were placed on top of homogeneous targets. Buschow *et al.* have studied samples with $30 \leq x \leq 90$ made by co-evaporation of Fe and B.[10] In this work, the magnetic properties and hyperfine interactions of amorphous Fe_xB_{100-x} will be presented for samples with Fe concentration up to 90 at.%. The properties of the nonmagnetic samples towards the pure B end will be discussed elsewhere.

II. EXPERIMENTAL

The amorphous Fe-B samples have been made by a high-rate sputtering device with Ar as the sputter gas. Vacuum in the chamber prior to throttling is in the mid-10^{-8}-Torr range. Cosputtering from two elemental targets of pure Fe and pure B had been originally considered but was found to be unacceptable due to difficulties in maintaining steady relative sputtering rates better than a few percent during the entire sputtering run without sophisticated feedback mechanisms. Rate control over two deposition sources is particularly important for amorphous Fe-B since the magnetic and other properties change greatly even for a few atomic percent difference in sample composition. Instead, each sample was sputtered from a *single* homogeneous target made from appropriate amounts of Fe and B. The sputtering rates were about 0.1 μm/min at a target to substrate distance of about 10 cm. A shutter was placed between the sputtering gun and the substrate platform during the presputtering period which was typically 30 min to 1 h. The film thickness ranges from 5 μm to a few tens of μm.

As in all vapor-deposition processes, adhesion of a relative thick film (greater than a few μm) is a troublesome problem. Adhesion depends on the deposition process and material deposited, as well as sub-

strates and substrate conditions.[3] The choice of substrate also depends on the measurements intended. Resistivity measurements, for example, require insulating substrates. For the ^{57}Fe Mössbauer measurements, the substrate must be reasonably transparent to the 14.4-keV γ ray unless the film can be removed from the substrate. To achieve adhesion and to satisfy the experimental requirements, we have used metal blocks, films of various metals deposited prior to the sputtering of the sample, insulating wafers, and synthetic polymers as substrate materials. In some cases, particularly for the thicker samples, the films can be removed from the substrates via thermal shock treatment or by mechanical means.

Sufficient substrate cooling is of considerable importance in making amorphous metallic solids for they crystallize at elevated temperatures.[2] Due to secondary electron bombardment during the sputtering process, the actual temperature of the film can be higher than the substrate temperature.[3] Most of the samples have been made with liquid-nitrogen-cooled substrates, although for samples with less than about 60 at.% Fe water-cooled substrates are adequate.

Toward the B-rich end, the amorphous state is readily formed with no apparent limitation on the compositions. However, at the Fe-rich end, there is an experimental limit on the Fe content. For a liquid-nitrogen-cooled substrate, amorphous samples could be obtained up to a Fe content of 90%. Our preliminary measurements indicate that the crystallization temperature of the Fe-rich samples decreases rapidly with increasing Fe concentration. Consequently, the samples with $x \geq 92$, when examined at room temperature, are partially or completely crystalline.

The composition and the amorphicity of some of the samples have been independently confirmed by Auger analyses and x-ray diffraction, respectively. Crystalline phases, if present, can also be readily detected from their physical properties, since the crystalline compounds of FeB, Fe_2B, Fe_3B, and α-Fe have distinctive magnetic ordering temperatures and Mössbauer spectra.[4,11,12]

Conventional ^{57}Fe Mössbauer spectroscopy has been employed with a ^{57}Co in Rh radioactive source. The measurements at 4.2 K have been made with the samples immersed in liquid helium. The measurements at elevated temperatures have been made in an oven in vacuum of 10^{-6} Torr.

III. RESULTS AND DISCUSSIONS

A. Magnetic ordering temperature (T_C)

The magnetic ordering temperatures (T_C) of the samples have been measured by the onset of the magnetic hyperfine interaction. This is conveniently accomplished by the thermal scan method, the details of which have been described elsewhere.[13] The values of T_C as a function of Fe content are shown in Fig. 1. The samples with low Fe content ($x \leq 35$) are not magnetic at 4.2 K. Their spectra show quadrupole-split doublets. The samples with $x \geq 40$ are magnetic at 4.2 K and their measured T_C are shown in Fig. 1. By extrapolation, the critical Fe concentration is about $x_c \simeq 38$, above which magnetic ordering occurs. Similar values of x_c have been found in amorphous Fe-Si, Fe-Ge, and Fe-Sn alloys.[14–16]

The existence of a critical concentration x_c is expected from a magnetic system in which the magnetic species are diluted by the nonmagnetic ones. The percolation theories predict a well-defined percolation threshold x_c, which is sensitively dependent on the nearest-neighbor coordination number (z), dictated by the structure.[17] These calculations usually assume magnetic moments of a fixed value, and the threshold is the result of percolation of the magnetic network. It is generally true that the larger the value of z, the smaller the value of x_c. The value of $x_c \simeq 38$ for amorphous Fe-B is higher than the values of 15–20 calculated from structures with high z.[18] While it is possible that for amorphous Fe-B near x_c, the coordination number is exceptionally low, a more likely cause for the high value of x_c is suggested by the magnetic data as described below.

Above x_c, the value of T_C rises sharply and at an approximately linear rate of about 40 K/at.%. A maximum is reached near $x = 70$, above which T_C *decreases* monotonically. This unusual behavior of decreasing T_C with increasing Fe concentration is particularly perplexing. If one takes the view of localized moments, T_C gives a measure of the net magnetic exchange interaction which is clearly decreasing. This can be due to a decrease of the ferromagnetic interaction or the emergence of antiferromagnetic interac-

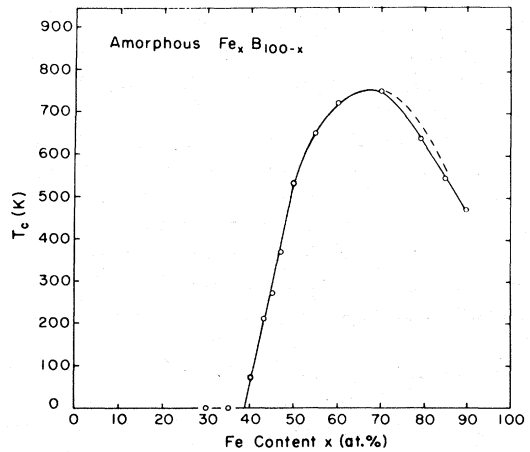

FIG. 1. Concentration dependence of the magnetic ordering temperature of amorphous Fe_xB_{100-x}.

tions. The observed high-field susceptibility and Invar characteristics in the Fe-rich samples are consistent with this assertion.[5,6] On the other hand, Wohlfarth *et al.* have argued that the itinerant electron model also predicts these properties.[18] In addition, however, the itinerant model predicts a similar decrease in the Fe moment, which is not observed in the present work, at least up to the concentration studied here. In fact, according to this model, amorphous pure Fe would be nearly or completely nonmagnetic with negligible moment and T_C.[19]

B. Hyperfine interactions

Mössbauer spectra of amorphous Fe-B at 4.2 K are shown in Fig. 2. As previously mentioned, samples with $x \leq 35$ are nonmagnetic and exhibit only a quadrupole doublet. Samples with $x \geq 40$ exhibit magnetic hyperfine patterns. The magnetic hyperfine splitting increases monotonically with increasing Fe concentration.

For many of the samples, due to substrate effects, the magnetic moments tilt out of the sample plane at low temperatures. Consequently, the No. 2 and No. 5 line intensities are suppressed as shown in Fig. 2. This effect in fact improves the resolution of the spectra. However, a small external field of about 1 kOe applied in the sample plane substantially aligns the moments back into the sample plane as shown in Fig. 3. The ease with which the Fe moments respond to a small field suggests that all of these samples are ferromagnetic and rather soft. Furthermore, there is increasing evidence to indicate that the tilting of the magnetic moments of low temperatures is caused by stresses from the substrate (presumably due to mismatch in the thermal expansion coefficients) or other external sources (e.g., adhesive tapes bonded onto the sample) via magnetostriction.[20] Thus, the fact that under stress the moments tilt substantially out of the sample plane also points to the ferromagnetic characteristics of the samples.

The hyperfine field distribution $\{P(H)\}$ of the spectra at 4.2 K have been analyzed using the Fourier-series method.[21] The effective quadrupole interaction is assumed to be negligible. This approximation is better justified when the magnetic hyperfine interaction is much larger than the quadrupole interaction. The value of b in the intensity ratio $3:b:1$ for the spectral lines is not presupposed but allowed to vary through successive iterations. For each spectrum, there is a unique b value which gives a minimum in the χ^2 as shown in Fig. 4. The $P(H)$ which corresponds to the uniquely defined b value is then used. As shown in Fig. 4, in the case of a-$Fe_{70}B_{30}$, with the application of an external field of about 1 kOe, the b value increases from 0.8 to 3.8, indicating a nearly complete alignment of the moments.

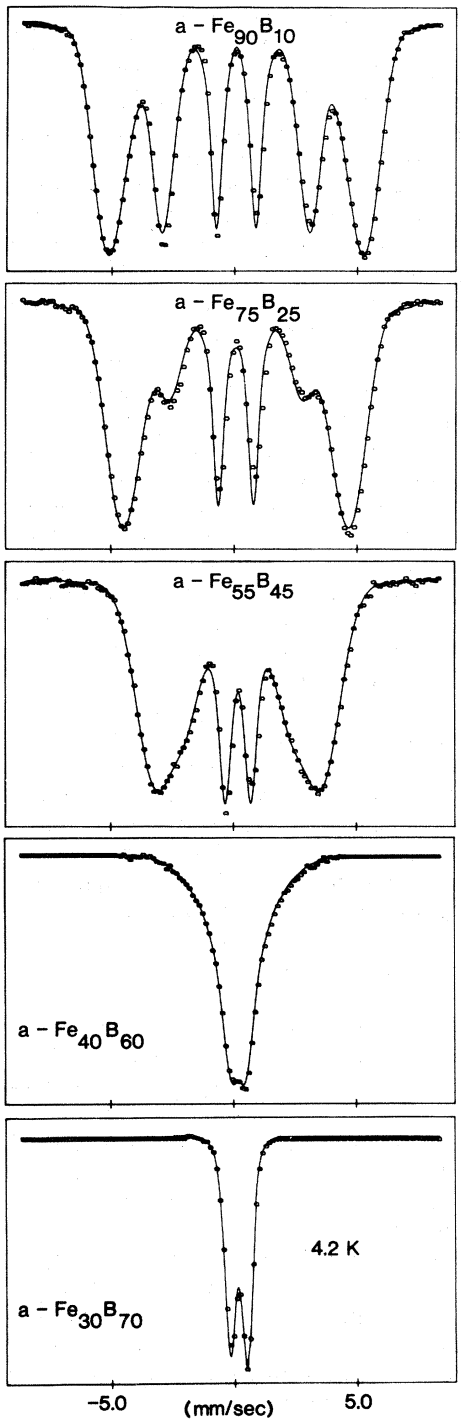

FIG. 2. Mössbauer spectra of amorphous Fe-B at 4.2 K.

The $P(H)$ of amorphous Fe-B are shown in Fig. 5. For clarity, not all the $P(H)$ are shown. The $Fe_{40}B_{60}$ sample shows a small and poorly resolved magnetic hyperfine splitting. Its spectrum at $T < T_C$ (e.g., at 4.2 K, Fig. 2) is clearly different from a quadrupole-split doublet spectrum (similar to the spectrum of

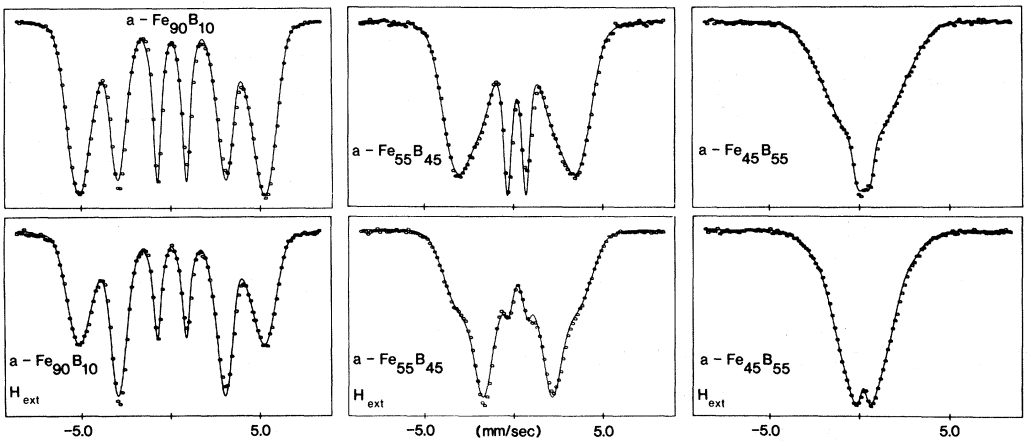

FIG. 3. Mössbauer spectra of amorphous $Fe_{90}B_{10}$, $Fe_{55}B_{45}$, and $Fe_{45}B_{55}$ without (top) and with (bottom) an external field of about 1 kOe applied in the sample plane.

$Fe_{30}B_{70}$ shown in Fig. 2) observed at $T > T_C$. However, the approximation of negligible effective quadrupole interaction is particularly poor. Therefore, the deduce $P(H)$ for $Fe_{40}B_{60}$ probably does not meaningfully represent the hyperfine field distribution.

The $P(H)$ of amorphous Fe-B are rather structureless. As the Fe concentration is increased, the $P(H)$ progressively and continuously shifts to higher H values. From the resultant $P(H)$, one can calculate the mean hyperfine field, defined as

$$H_{\text{mean}} = \int P(H) H \, dH \quad . \tag{1}$$

As shown in Fig. 6, H_{mean} increases monotonically with Fe content, despite the fact that there is a maximum in T_C. The mean hyperfine fields for crystalline Fe-B compounds and amorphous alloys of the same composition are rather similar.

It has been shown in crystalline Fe-B compounds and liquid-quench amorphous solids that H_{mean} is, to a good approximation, proportional to the mean Fe moment as determined from magnetization and neutron-diffraction measurements.[4] With this assumption, Fig. 6 indicates that the Fe moment likewise increases sharply with Fe concentration. Very recently, Buschow *et al.* have studied the magnetization of amorphous Fe-B samples.[10] The Fe moment indeed increases sharply with increasing Fe content.

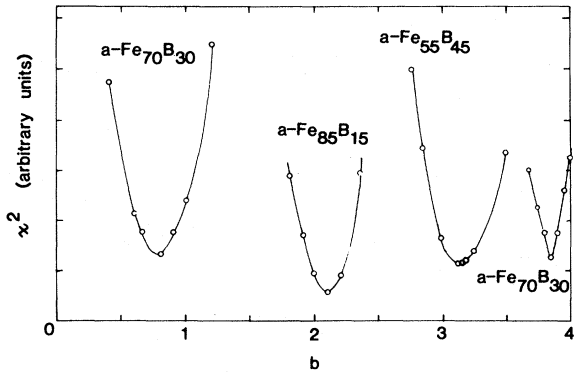

FIG. 4. Quality of fit (χ^2) as a function of b which is the intensity of the No. 2 and No. 5 peak of the spectrum.

It is particularly interesting to note that H_{mean}, and thus the Fe moment vanishes near $x = 38$, which is precisely the percolation-like threshold x_c as determined from T_C (Fig. 1). This indicates that the high value of the threshold concentration at $x_c \simeq 38$ is caused by the vanishing Fe moments *before* the expected percolation threshold (assuming nonvanishing moments) is reached at a lower Fe concentration.

Our preliminary results on the amorphous Ni-B and Co-B systems, together with the results on Ni-P by Barada *et al.* indicate that the percolation-like thresholds are very much different for Ni-metalloid and Co-metalloid glasses.[22] These results suggest that the magnetic moments of the transition-metal elements are not constants but are strongly dependent on the metal and metalloid concentration.

The evolution of the value of the Fe moment and its disappearence in crystalline and amorphous alloys has been discussed in the literature. In the nearest-neighbor coordination model,[14,23] it is assumed that the Fe moment depends on the number of Fe atoms and metalloid atoms in the first nearest-neighbor (NN) shell. When the NN Fe coordination number falls below a certain value, the Fe atom ceases to have a moment. Under this model, the value of the Fe moment in amorphous Fe-B would increase monotonically. Despite its *"ad hoc"* nature, this model does qualitatively account for the experimental results.

In the itinerant model, the decrease and the disappearance of the Fe moment is simply a band-filling ef-

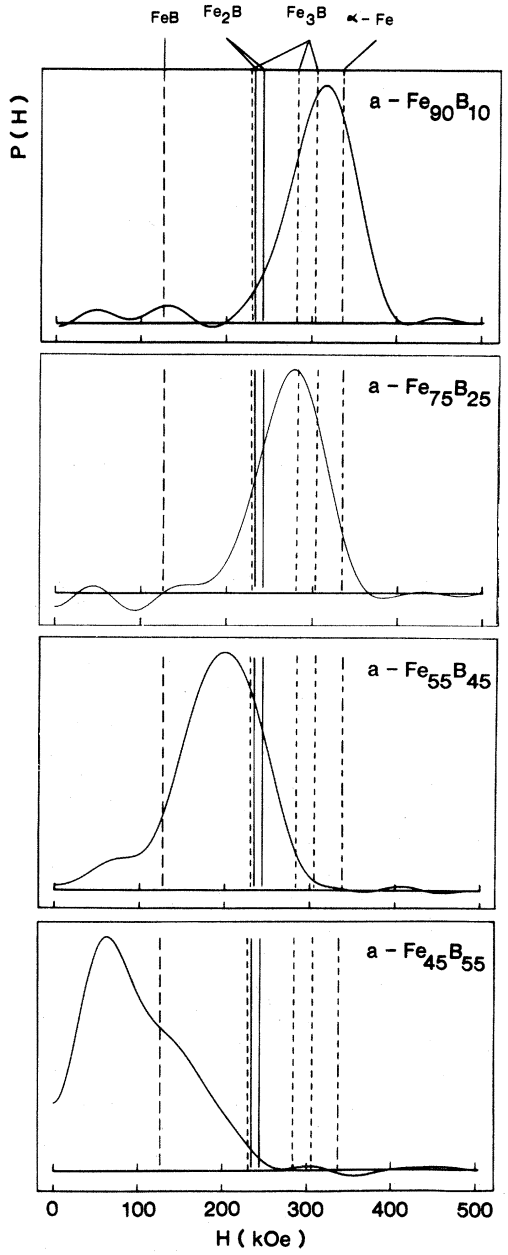

FIG. 5. Hyperfine field distributions $\{P(H)\}$ of amorphous Fe-B. The vertical solid lines and dashed lines are the field values of crystalline FeB, Fe_2B, Fe_3B, and α-Fe.

fect, in which the metalloid transfers electrons to the metal d band.[18,19,24] In the Fe-rich end, the itinerant model predicts a decrease in both T_C and the Fe moment as previously mentioned. The former is experimentally observed whereas the latter is not. It is of course possible that the moment decreases at an Fe concentration which is higher than 90 at.%.

The isomer shifts of the amorphous Fe-B samples at 4.2 K are shown in Fig. 7. The most unusual

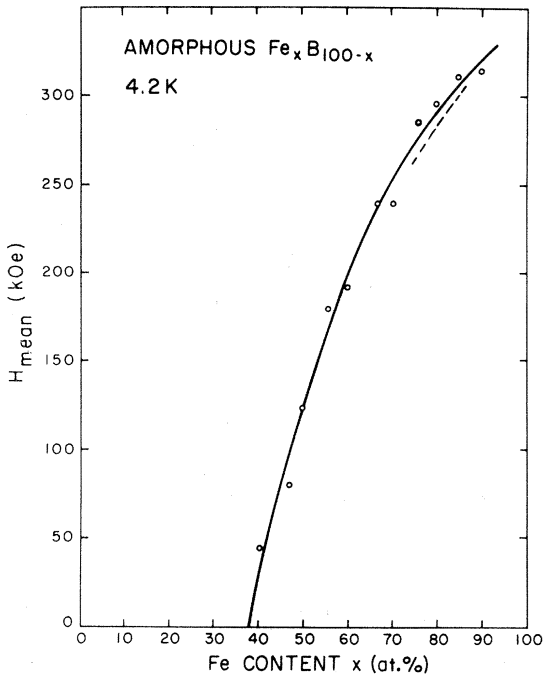

FIG. 6. Mean hyperfine field of amorphous Fe-B as a function of Fe concentration.

feature displayed is that the isomer shifts of the Fe-rich samples and the Fe-poor samples have opposite concentration dependences. Consequently, a maximum in the isomer shift occurs near $x = 50$.

To account for the isomer shifts dependence on Fe concentration in the liquid-quench samples with $72 \leq x \leq 86$, a charge transfer or donor model has been suggested. In this model, one assumes that boron transfers charge to the Fe d band. In its simplest form, the isomer shift varies with Fe concentration (x) via the relation[25]

$$\delta(x) = \delta_0 + D\left(\frac{100-x}{x}\right) , \tag{2}$$

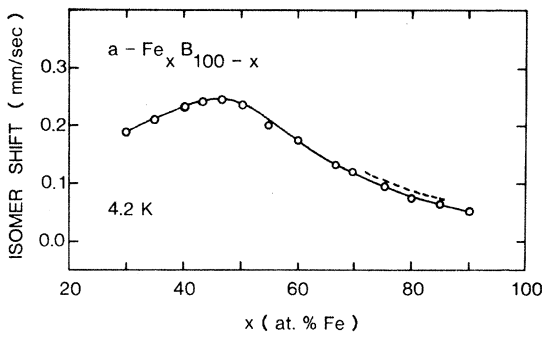

FIG. 7. Isomer shift of amorphous Fe-B at 4.2 K as a function of Fe concentration.

where δ_0 is the isomer shift of metallic Fe and D is a constant.

For the present data, isomer shifts of the Fe-rich samples can be well described by Eq. (2) with a value of $D = 0.27$ mm/sec. The dependence predicted by Eq. (2) begins to deviate from the experimental data at about $x = 70$ and becomes progressively worse for lower x. Since Eq. (2) is a monotonic function of x, it would never predict a maximum in the isomer shift as experimentally observed.

It is clear that the isomer shifts observed in amorphous Fe-B over a wide concentration range cannot be accounted for by a simple charge transfer model. From the data shown in Fig. 7, it appears that there are two main contributions to the variation of isomer shift. One increases while the other decreases with Fe concentration. A maximum in the isomer shift is a reflection of these opposite trends.

C. Comparison with liquid-quench samples ($72 \leq x \leq 86$)

Since the quenching rates for the liquid-quench and vapor deposition processes are different, it is of interest to compare the present results with those of liquid-quench samples with $72 \leq x \leq 86$. In Figs. 1, 6, and 7 we show the results of the liquid-quench samples, which we have reported previously, by the dotted curves.[4] It appears that the sputtered samples have a lower T_C, larger hyperfine field, and a smaller isomer shift. These differences, however, may or may not be due to the possible structural differences of the samples made by different techniques for the following reasons. If one is certain about the compositions of the sputtered samples and the liquid-quench samples to an absolute accuracy of better than 1 at.%, then the observed differences between these two sets of samples represent their quenching rates difference. On the other hand, a closer examination of Figs. 1, 6, and 7 shows that the observed differences between the two sets of samples can be reconciled if there is a consistent composition difference of only *2 at. %* between the two sets of samples. In microanalyses of sample compositions, because of the low atomic number of boron, while the relative accuracy is high, the absolute accuracy with which the compositions can be determined is only a few atomic percent. At any rate, the present comparison shows that the differences, if any, between the liquid-quench and the sputtered samples are rather small.

D. Microcrystalline and quasicrystalline models

Since x-ray diffraction measurements have a limited resolution, a microcrystalline model was proposed some years ago, shortly after the amorphous metallic solids were made.[26] In this model, the amorphous solid is assumed to be made of small crystallites, tens of angstroms in size, which are not revealed by x-ray diffraction. However, microscopic measurements, such as Mössbauer spectroscopy, on ultrafine crystalline particles, 50–100 Å in size, show that the results at low temperatures (to suppress superparamagnetism) essentially exhibit all the characteristics of the bulk material.[27] Therefore, if amorphous Fe-B alloys were made of microcrystallites, their spectra would show sharp spectral lines corresponding to the hyperfine fields of the crystalline compounds of 131 kOe (FeB); 242 and 252 kOe (Fe_2B); 242, 284, and 305 kOe (Fe_3B); and 341 kOe (α-Fe). As shown in Figs. 2 and 5, this is clearly not observed in the spectra or the $P(H)$.

The saturation H values of crystalline FeB, Fe_2B, Fe_3B, and α-Fe are shown in Fig. 5 by the vertical lines. It is noted that the $P(H)$ of the liquid-quench samples with $72 \leq x \leq 86$ envelopes the H values of crystalline Fe_3B (in fact, also those of crystalline Fe_2B and α-Fe). This observation led to the "quasicrystalline" model proposed by Vincze *et al.*[28] This model is based on the claim that the $P(H)$ of the liquid-quench samples with $72 \leq x \leq 86$ can be reasonably reproduced by adjusting the weights of three broad Gaussian distributions centered about the three H values of Fe_3B. The implications are that the short-range order is essentially the same in crystalline and amorphous solids. Furthermore, structural disorder with respect to the crystalline solid is small (about 10%).

One notes, however, that all but one of the H values of the crystalline Fe-B compounds are from 242 to 341 kOe, which are enveloped by the $P(H)$ of the liquid-quench samples. Thus the liquid-quench samples do not provide a wide enough composition range to conclusively test the "quasicrystalline" model. A more useful test is to examine the $P(H)$ of samples with x less than 70, where the $P(H)$ do not overlap substantially with the crystalline H values. Since there is only one H value of 131 kOe between 0 and 242 kOe, the validity of the model can be directly tested.

One such example is shown in Fig. 5 for $Fe_{55}B_{45}$. Its $P(H)$ peaks at a value which does not coincide with any crystalline H values. Its simple shape cannot be reproduced by broad Gaussians at the crystalline H values either. Furthermore, the $P(H)$ of amorphous Fe-B shifts continuously as the Fe content is varied without irregularity at the crystalline H values. Thus, when the amorphous Fe-B solids are examined as a whole, the "quasicrystalline" model is not applicable. There are also indications that for sample with x as high as 70 the prediction of this model is already quite poor.[29] One suspects, even for samples near $Fe_{80}B_{20}$, for which the model was first proposed, it is the presence of a large number of crystalline H values which helps to reproduce the $P(H)$ of the amorphous counterparts.

IV. CONCLUSIONS

In conclusion, the magnetic ordering temperatures, hyperfine interactions, and isomer shift systematics have been determined for amorphous Fe-B samples near and above the percolation-like threshold at $x_c \simeq 38$. T_C exhibts a maximum at about $x = 70$, the general features of which can be explained from both the localized and itinerant pictures. However, the itinerant model also predicts a maximum in the Fe moment which is not observed up to the highest Fe concentration studied.

The $P(H)$ show simple single-maximum patterns which continuously shift to higher H values for increasing Fe concentration. The average Fe moment, as deduced from the $P(H)$ and confirmed by recent magnetization measurements, is not constant but increases monotonically. It is evident that the percolation-like behavior at $x_c \simeq 38$ is driven by the diminishing moments and is not a true percolation limit. The $P(H)$ for samples with x less than 70 cannot be reproduced by sums of Gaussians centered about the crystalline H values. The experimental evidence therefore, does not support the micro- and quasicrystalline models of amorphous structure.

The fact that the isomer shift shows a maximum near $x = 50$ indicates at least two contributions of opposite signs to the isomer shift. This behavior cannot be accounted for by a simple charge transfer model which predicts a monotonic change.

We have observed slight differences between the sputtered and the liquid-quench samples in the range of common compositions of $72 \leq x \leq 86$. However, these deviations can be reconciled if the compositions of either set of samples are different from their nominal values by only 2%.

ACKNOWLEDGMENTS

This work is supported by the NSF Grant No. DMR79-10536. We thank Professor E. P. Wohlfarth for interesting discussions and manuscripts prior to publication.

[1]P. Duwez, Trans. Am. Soc. Met. 60, 607 (1967).
[2]H. S. Chen, Rep. Prog. Phys. 43, 353 (1980), and references therein.
[3]See, e.g., *Thin Film Processes,* edited by C. J. Vossen and W. Kern (Acadamic, New York, 1980).
[4]C. L. Chien, D. Musser, E. M. Gyorgy, R. C. Sherwood, H. S. Chen, F. E. Luborsky, and J. W. Walter, Phys. Rev. B 20, 283 (1979).
[5]K. Fukamichi, M. Kikuchi, S. Arakawa, and T. Masumoto, Solid State Commun. 23, 955 (1977).
[6]H. Hiroyoshi, K. Fukamichi, M. Kikuchi, A. Hoshi, and T. Masumoto, Phys. Lett. 65A, 163 (1978).
[7]J. A. Aboaf, R. J. Kobliska, and E. Klokholm, IEEE Trans. Magn. 14, 941 (1978).
[8]N. A. Blum, K. Moorjani, T. O. Poehler, and F. G. Satkiewicz, J. Appl. Phys. 52, 1808 (1981).
[9]T. Stobiecki and H. Hoffman, J. Phys. (Paris) 41, 485-C8 (1980).
[10]K. H. J. Buschow and P. G. van Engen, J. Appl. Phys. 52, 3557 (1981).
[11]J. B. Jeffries and N. Hershkowitz, Phys. Lett. 30A, 187 (1969).
[12]K. A. Murphy and N. Hershkowitz, Phys. Rev. B 7, 23 (1973).
[13]C. L. Chien and K. M. Unruh, Phys. Rev. B 24, 1556 (1981).
[14]G. Marchal, Ph. Mangin, M. Piecuch, Chr. Janot, and J. Hubsch, J. Phys. F 7, L165 (1977).
[15]G. Suran, H. Daver, and J. C. Bruyer, in *Magnetism and Magnetic Materials—1975,* edited by J. J. Becker and G. H. Lander, AIP Conf. Proc. No. 29 (AIP, New York, 1975), p. 162.
[16]B. Rodmacq, M. Piecuch, Chr. Janot, G. Marchal, and Ph. Mangin, Phys. Rev. B 21, 1911 (1980).
[17]J. W. Essam, in *Phase Transitions and Critical Phenomena,* edited by C. Domb and M. S. Green (Academic, New York, 1972), Vol. 2.
[18]F. E. Luborsky, J. L. Walter, and E. P. Wohlfarth, J. Phys. F 10, 959 (1980).
[19]E. P. Wohlfarth (unpublished).
[20]H. N. Ok and A. H. Morrish, Phys. Rev. B 22, 4215 (1980).
[21]C. L. Chien, D. Musser, F. E. Luborsky, and J. L. Walter, J. Phys. F 10, 2407 (1978).
[22]A. Berrada, F. Gautier, M. F. Lapierre, B. Loegel, P. Panissod, and C. Robert, Solid State Commun. 21, 671 (1977).
[23]V. Jaccarino and L. R. Walker, Phys. Rev. Lett. 15, 258 (1965).
[24]See, e.g., T. Mizoguchi, in *Magnetism and Magnetic Materials—1976,* edited by J. J. Becker and G. H. Lander, AIP Conf. Proc. No. 34 (AIP, New York, 1976), p. 286.
[25]L. Takacs, in Conference on Soft Magnetic Materials, Bratislava, 1977 (unpublished).
[26]See, e.g., G. S. Cargill, Solid State Phys. 30, 227 (1975).
[27]T. K. McNab, R. A. Fox, and A. J. F. Boyle, J. Appl. Phys. 39, 5703 (1968).
[28]I. Vincze, D. S. Boudreaux, and M. Tegze, Phys. Rev. B 19, 4896 (1979).
[29]A. S. Schaafsma, I. Vincze, and F. van der Woude, J. Phys. (Paris) 41, 246-C8 (1980).